Front. Mater. Sci. 2016, 10(1): 90–100
DOI 10.1007/s11706-016-0329-9

RESEARCH ARTICLE

In vitro evaluation of electrospun gelatin–glutaraldehyde nanofibers

Jianchao ZHAN[1,2], Yosry MORSI[3], Hany EI-HAMSHARY[4,5], Salem S. AL-DEYAB[4], and Xiumei MO (✉)[1]

1 College of Chemistry, Chemical Engineering and Biotechnology, Donghua University, Shanghai 201620, China
2 College of Materials and Textile Engineering, Jiaxing University, Jiaxing 314001, China
3 Faculty of Engineering and Industrial Sciences, Swinburne University of Technology, Hawthorn, Vic 3122, Australia
4 Department of Chemistry, College of Science, King Saud University, Riyadh 11451, Saudi Arabia
5 Department of Chemistry, Faculty of Science, Tanta University, Tanta 31527, Egypt

© Higher Education Press and Springer-Verlag Berlin Heidelberg 2016

ABSTRACT: The gelatin–glutaraldehyde (gelatin–GA) nanofibers were electrospun in order to overcome the defects of *ex-situ* crosslinking process such as complex process, destruction of fiber morphology and decrease of porosity. The morphological structure, porosity, thermal property, moisture absorption and moisture retention performance, hydrolytic resistance, mechanical property and biocompatibility of nanofiber scaffolds were tested and characterized. The gelatin–GA nanofiber has nice uniform diameter and more than 80% porosity. The hydrolytic resistance and mechanical property of the gelatin–GA nanofiber scaffolds are greatly improved compared with that of gelatin nanofibers. The contact angle, moisture absorption, hydrolysis resistance, thermal resistance and mechanical property of gelatin–GA nanofiber scaffolds could be adjustable by varying the gelatin solution concentration and GA content. The gelatin–GA nanofibers had excellent properties, which are expected to be an ideal scaffold for biomedical and tissue engineering applications.

KEYWORDS: nanofiber; electrospinning; gelatin; tissue engineering

Contents

Received October 19, 2015; accepted December 7, 2015

E-mail: xmm@dhu.edu.cn

1 Introduction

Electrospinning is a simple, economical and effective method to prepare continuous micro-nanofiber. Electrospun nanofiber scaffold has exceedingly high surface area to volume, which is conducive to material–cell interaction and cell growth and reproduction. Therefore, it is considered as potential tissue engineering material [1–3]. Electrospun gelatin nanofiber is characteristic of low cost, good biocompatibility, non-cytotoxicity, no antigenicity, structure and functional resemblance with natural extracellular matrix (ECM). Its use in tissue engineering, drug delivery and wound dressing draws the attention of scientific community [4–10]. However, the applications of electrospun gelatin nanofiber are limited by its quick degradation or poor mechanical property. Thus further treatment to enhance its stability in water medium such as crosslinking is required. Crosslinking agents such as glutaraldehyde (GA), glyceraldehyde, genipin, carbodiimide, epichlorohydrin [11–14], procyanidine [9–15], sodium polymetaphosphate [16], modified glucan [17] and oxidized sucrose [18] are commonly being used for gelatin nanofibers. GA is inexpensive and high crosslinking efficiency, which can greatly enhance hydrolysis resistance and mechanical property of gelatin nanofibers, and hence it is the most common crosslinking agent. Crosslinked gelatin nanofiber scaffold by *ex-situ* process is prepared in two-step process: an aqueous gelatin solution is electrospun to prepare gelatin nanofiber membranes, and then the membranes are crosslinked in GA solution or vapor. The features of this *ex-situ* process are mainly non uniform (only in the surface layer of fiber or fibrous scaffold) and severe fusion of fiber during crosslinking which considerably brings down porosity of the scaffold [11–18]. Therefore, it is indispensable to develop a new and convenient crosslinking method for gelatin nanofiber. Tang et al. have reported an *in-situ* process to produce crosslinked poly(vinyl alcohol) (PVA) nanofiber membrane by incorporating GA and a strong acid (HCl) into the electrospinning solution immediately before processing [19]. Cao et al. have taken the *in-situ* process to prepare crosslinked gelatin nanofibers membrane [20]. In this work, gelatin–GA nanofibrous scaffolds were prepared by electrospinning. The mechanical, chemical and biological properties of the gelatin–GA nanofiber scaffolds were evaluated.

2 Experimental

2.1 Materials

Deep sea fish skin gelatin, biological reagent (BR), Canada Sigma. GA, BR, Sinopharm Chemical Reagent Beijing Co., Ltd. Dimethyl sulfoxide (DMSO), phosphate buffer saline (PBS, pH = 7.4), hexafluoroisopropanol (HFIP), Sigma-Aldrich. L929 cells, College of Biochemistry and Cell Biology, Shanghai Institute for Life Sciences of Chinese Academy of Sciences. 3-(4,5-Dimethyl-2-thiazolyl)-2,5-diphenyl-2-H-tetrazolium bromide (MTT), fetal calf serum (FCS), double resistant and Dulbecco modified Eagle medium (DMEM) nutrient solution, Gibco.

2.2 Preparation of gelatin–GA nanofibers

The preparation process is illustrated in Fig. 1. Gelatin was dissolved in HFIP to prepare gelatin solution with concentration of 6 wt.%, 7 wt.% and 8 wt.% respectively, and stirred at 50°C for 6 h. GA solution (2.5 wt.%) was dripped into the gelatin solution according to the *w*(GA)/*w*(gelatin) mass ratio of 1/400 and 1/300 respectively and stirred continuously for 8 h. With applied voltage of 13 kV, flow rate of 0.9 mL/h and collecting distance of 20 cm, gelatin–GA solution was electrospun to prepared crosslinked nanofiber scaffolds by varying the gelatin and GA concentrations. In addition, gelatin nanofiber scaffolds were successfully fabricated at the concentration of 12% (g/mL, using HFIP as solvent) via electrospinning.

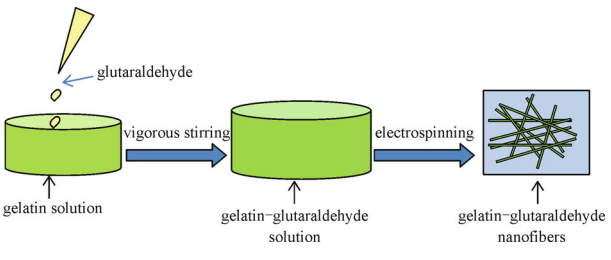

Fig. 1 Preparation process of gelatin–GA nanofiber scaffolds.

2.3 Test and representation

2.3.1 Characterizations

Morphology of the nanofiber was investigated by scanning electron microscopy (SEM, JSM-5600, Japan). After sputter-coated with platinum on the surface of samples, the morphology was observed by SEM at the accelerating voltage of 10 kV. Diameter distributions of the sample were determined using Image J by randomly selecting 100 fibers. The infrared spectra of the dried samples in KBr discs were confirmed by using a Fourier transform infrared spectroscopy (FTIR) spectrophotometer (NEXUS-670, USA). The tested wave number range is 500–4000 cm^{-1}, and the interval is 4 cm^{-1}. The uncrosslinked gelatin nanofiber scaffold was used as a control. The X-ray diffraction (XRD) pattern of sample was tested by using a D/max-2550PC rotating anode X-ray diffractometer. The tube voltage is 40 kV, the tube current is 300 mA and the scanning speed is 6(°)/min. Calorimetric measurements were performed using a NETZSCH DSC200PC to determine the change in crystallinity of samples. The sample weights were in the range of 4–6 mg. Samples were examined in air-dried conditions. Heating was carried out at 10°C/min from 30°C to 250°C.

2.3.2 Mechanical property test

The samples were cut into rectangular strips with thickness of 0.035 mm (area: 50 mm × 10 mm). The mechanical property of nanofiber scaffolds was tested with materials testing machine (H5K-S, Hounsfield, UK) at stretching velocity of 10 mm/min, at 20°C with humidity of 65%.

2.3.3 Contact angle measurement

OCA40 contact angle meter was applied to test the contact angle of water drop and sample surface when the deionized water was dropped on the surface of dry samples for 5 s. The hydrophilic and hydrophobic property of sample was observed.

2.3.4 Water uptake and moisture retention test

A piece of nanofiber scaffold (20 mm × 20 mm) was cut and precisely weighed (denoted as W_0). Then, it was dipped into a small beaker of PBS solution (37°C, 50 mL) for a while before being carefully taken out with tweezers. The water on the surface was absorbed with filter paper and then the wet weight is obtained (denoted as W_1). The water uptake, η_{wu}, was calculated according to Eq. (1):

$$\eta_{wu}/\% = \frac{W_1 - W_0}{W_0} \times 100 \quad (1)$$

After saturation with water, it was centrifuged for 3 min at the speed 500 r/min, and precisely weighed (denoted as W_s). Then, the sample was put into the constant temperature incubator with temperature of 37°C and relative humidity of (39±1)%. It was weighed every other 30 min (denoted as W_t). The water evaporation rate, η_{wer}, was calculated according to Eq. (2):

$$\eta_{wer}/\% = \frac{W_s - W_t}{W_s - W_0} \times 100 \quad (2)$$

The water absorption and water retention performance of scaffold are obtained by taking the mean value of six data of each electrospun nanofiber scaffold.

2.3.5 Degradation property

A piece of nanofiber scaffold was cut into rectangular samples (3 cm × 6 cm). The samples were weighed (denoted as W_f) and dipped into sample bottle of PBS solution (20 mL) one by one. Sodium azide was put into the PBS solution according to 2 mg/mL. The sample bottle was put into constant temperature shaker incubator (37°C), with the PBS solution being replaced every one week. At each appointed point-in-time, the sample was deprived of deionized water, washed and then freeze dried and weighed (denoted as W_b). The weight loss rate, η_{wlr}, was calculated according to Eq. (3):

$$\eta_{wlr}/\% = \frac{W_f - W_b}{W_f} \times 100 \quad (3)$$

2.3.6 Biocompatibility *in vitro*

The petri dish which held L929 cells and DMEM culture medium with 10% of FCS and 1% of double resistant was put into the incubator (37°C, humidity of 95%, with 5% of CO_2), and the nutrient solution was replaced every third days. The round cover glass (with diameter of 14 mm) which carried nanofiber scaffold was put into a 24-well culture plate (1 sample in 1 well) and pressed with a stainless steel ring above. Before cell seeding, the nanofiber scaffold was disinfected with ethanol solution (75%) for 4 h and washed with PBS solution for three times. The sample was exposed to ultraviolet ray (230 V, 50

Hz) overnight. On the second day, the PBS solution was removed and DMEM culture medium with 10% of FCS and 1% of penicillin–streptomycin was put into the incubator. As the cell density reached 90% confluence, the cells were harvested and then seeded onto the scaffold at a seeding density of 1.0×10^4 per sample and cultivated in the incubator for 1, 3, 5 and 7 d.

The MTT method was used to evaluate the activity of cells on the nanofiber scaffold. 400 μL of DMEM and 40 μL of MTT (MTT 5 mg/mL) were put into each well and cultivated for 4 h under standard condition of culture. Then, all the nutrient solution was removed, 400 μL of DMSO was put into each hole and shaken in constant temperature incubator (37°C, 100 r/min) for 30 min to form purple solution. The solution was put into a 96-hole culture plate (100 μL/well), and its absorbance was measured with micro plate reader MK3 at the wavelength of 570 nm.

2.3.7 Statistical analysis

The results are represented with average value ± standard deviation. In comparative study, one-way analysis of variance is adopted. $p<0.05$ indicates a significant difference.

3 Results and discussion

3.1 Morphology analysis

When electrospinning voltage, receiving distance, flow rate and other technical parameters are fixed, the viscosity of polymer is the dominant factor which affects fiber morphology [21]. Under the electric field, low-viscosity spinning solution switches unsteadily, which results in large difference in levels of stretch and produces thin and non-uniform fibers. High-viscosity spinning solution is apt to form gel and spin unsteadily; therefore the produced fibers are thick and non-uniform. Moreover, owing to high viscosity, the solvent is hard to completely volatilize, so the fibers are apt to merge and bond. The morphological structures of gelatin–gelatin nanofiber with different gelatin concentration and GA content are shown in Fig. 2, and the average diameters of fibers are listed in Table 1. It shows that G64 (Fig. 2(a)) has a poor molding and the average diameter is 301 nm; G63 (Fig. 2(b)) is relatively smooth and the average diameter is 345 nm. G74 (Fig. 2(c)) and G73 (Fig. 2(d)) have good molding and even thickness, and the average diameter of G73 (992 nm) is slightly larger than that of G74 (885 nm). G84 (Fig. 2(e)) and G83 (Fig. 2(f)) are thick yet non-uniform, and G83 manifests merging and bonding. It can be seen that G74 and G73 have moderate concentration and GA content.

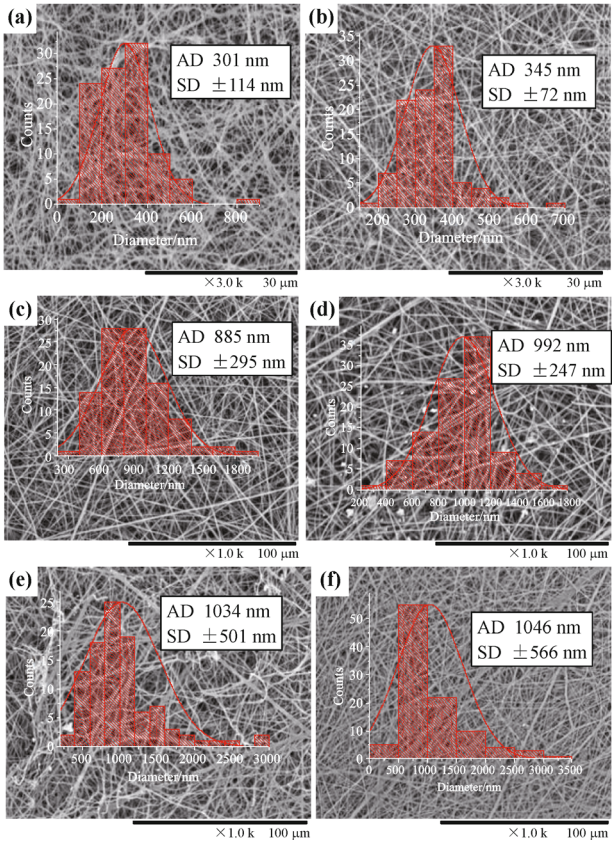

Fig. 2 SEM images of gelatin–GA nanofiber scaffolds and corresponding diameter distribution diagrams: **(a)** G64; **(b)** G63; **(c)** G74; **(d)** G73; **(e)** G84; **(f)** G83.

3.2 Porosity analysis

There should be a certain amount of interconnected cellular structures in scaffold for tissue engineering so as to support nutrient substance flow and oxygen exchange which is required by cell proliferation and tissue growth. Therefore, porosity is another important parameter for evaluating the scaffold for tissue engineering [22–23]. The porosity of gelatin–GA nanofiber scaffold is listed in Table 1 indicating that the porosity of all the nanofiber scaffolds is above 80%. It can be clearly seen that there are large pore structures between gelatin–GA nanofibers in Fig. 2. With the increase of GA, the free space in the scaffold shrinks owing to growing fiber diameter and fiber adhesion. The scaffold density grows and the specific surface area of fiber in the scaffold decreases, so the porosity goes down.

Table 1 The physical properties of gelatin–GA nanofiber scaffolds

Sample	w(GA) /w(gelatin) [a]	c(gel) /(g·mL^{-1}) [b]	δ_{fs} /mm [c]	d_f /nm [d]	ρ_{ave} /(g·cm^{-3}) [e]	φ /% [f]	σ_{bs} /MPa [g]	ε_{be} /% [h]	E /MPa [i]	$\eta_{wu,max}$ /% [j]
G64	1/400	6	0.035	301±114	0.182	86.52	1.375	3.56	0.537	265±5.5
G63	1/300	6	0.037	345±72	0.21	84.42	2.187	4.53	0.651	251±3
G74	1/400	7	0.037	885±295	0.211	84.38	4.24	5.02	1.648	413±6
G73	1/300	7	0.039	992±247	0.222	83.55	7.288	4.32	2.81	385±16
G84	1/400	8	0.032	1034±601	0.223	83.5	6.69	2.93	2.77	443±26
G83	1/300	8	0.035	1046±566	0.231	82.88	3.87	2.23	1.92	435±5.5

Note: The gelatin density is 1.35 g/cm^3.
a) Mass ratio; b) Gelatin concentration; c) Fibrous scaffold thickness; d) Fiber diameter; e) Average density; f) Porosity; g) Breaking strength; h) Breaking elongation; i) Young's modulus; j) Maximum water uptake.

3.3 Infrared spectroscopic analysis

FTIR spectra of gelatin nanofiber scaffolds are showed in Fig. 3. As can be seen, all spectra obtained are similar and exhibit the characteristic peaks of gelatin nanofibers. Compared with the gelatin nanofiber and the gelatin–GA samples, the large band (amide A) observed at 3409 cm^{-1} were associated with the stretching vibration of N–H group, the band (amide I) observed at 1644 cm^{-1} were based on coupled C=O stretching and C–NH bending, the band (amide II) observed at 1541 cm^{-1} represented the bending vibration of N–H group, the band observed at 1234 cm^{-1} were associated with the bending vibration of C–N group, and their intensity were observed relatively decreasing after crosslinking. There is crosslinking reaction between GA and $-NH_2$ in gelatin (Eq. (4)), so the NH_2 content in gelatin decreases after crosslinking and the more GA the higher decrease degree is. The absorption peak of amide I band in G64, G74 and G84 moves slightly towards high wave number from 1644 to 1649 cm^{-1}. The reason may be that with addition of little GA, the hydrogen-bond interaction of intra- and inter-molecular chain weakens and the amide I characteristic absorption peak of gelatin scaffold moves towards high wavenumber [24]. The absorption peak of amide I band in the G63, G73 and G83 moves towards low wavenumber from 1644 to 1622 cm^{-1}. The reason may be that the excess GA destroys the triple helix structure of gelatin, so hydrophilic free radicals increase and the hydrogen-bond interaction is boosted [25]. Equation (4) is as follows:

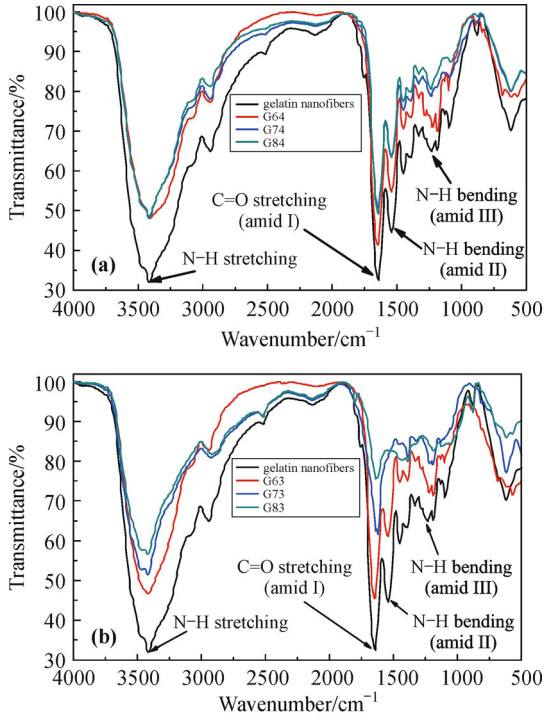

Fig. 3 FTIR spectra of gelatin–GA nanofibers with the mass ratio of w(GA)/w(gelatin) at **(a)** 1/400 and **(b)** 1/300.

$$GA–CHO + gelatin–NH_2 \rightarrow GA–C{=}N–gelatin \quad (4)$$

3.4 XRD analysis

XRD is used to study the crystallinity of gelatin electrospun nanofiber. The XRD patterns of the gelatin and gelatin–GA nanofiber scaffolds are shown in Fig. 4. It can be seen that, there are two diffraction peaks in the pattern of gelatin nanofiber scaffold. One is the crystalline diffraction peak near $2\theta = 8.4°$ which corresponds to triple helix structure, and the other is at 18.6° which corresponds to α-helical structure [26–27]. Although the triple helix is not tested quantitatively in this research, the result above shows that the triple helix is at least partly reserved after electrospinning. Figure 4 reveals that the patterns of G64, G74 and G84 are similar to that of gelatin nanofiber scaffold. It indicates that when GA content is low,

crosslinking in molecular chains has little destructive effect on the crystal, and the molecular chains crosslink, fix together and form zip structure. Therefore, the degree of crystallinity of gelatin nanofiber scaffold does not decrease but increases. The crystalline diffraction peaks at $2\theta = 8.4°$ of G63, G73 and G83 disappear, and the peaks near 18.6° diminish to a large margin. The cause may be, as gelatin and sufficient GA fully crosslink, the orientation of molecular chains is restrained, so the crystal face does not fully grow and the peak intensity weakens and tends to be non-crystalline structure.

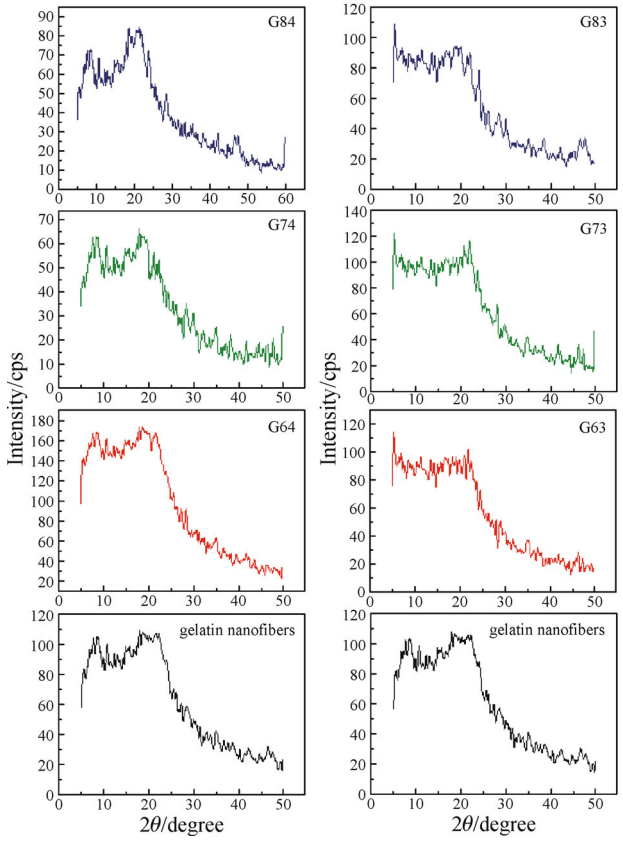

Fig. 4 XRD patterns of gelatin–GA nanofiber scaffolds.

3.5 Differential scanning calorimetry (DSC)

DSC analysis is carried out to the thermal property of gelatin–GA nanofiber scaffold. It can be seen in Fig. 5 that, there are two endothermic peaks on the DSC heat curve. One is at 88°C–110°C which is considered as temperature of protein degeneration caused by gelatin dehydration, hydrogen bond breakage and random recombination of triple helix [18,28–29]. The other is at 200°C–230°C which is consistent with the decomposition temperature of gelatin [30–32]. The peak temperatures of G64, G74, G84, G63, G73 and G83 are 86.03°C, 84.87°C, 87.17°C, 90.7°C, 88.07°C and 91.37°C, respectively. All of them are higher than the peak temperature of gelatin nanofiber, which is 83.2°C. It reveals that gelatin–GA nanofiber has better heat stability. The higher the GA content the better the heat stability. It is reported that gelatin and GA crosslink form –C=N– covalent bond and result in higher energy which is required by molecular chain breakage [33–36]. This research is consistent with this report.

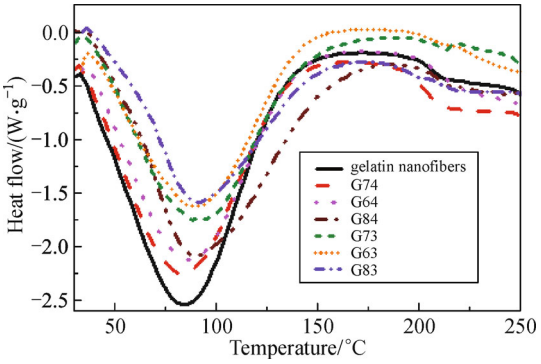

Fig. 5 DSC curves of gelatin–GA nanofiber scaffolds. All the samples possess a similar water content of 12 wt.%.

3.6 Water-holding capacity analysis

Scaffolds for tissue engineering with favorable water-holding capacity can not only absorb most of the wound exudate but also keep the environment moist so as to facilitate nutrient transport and cell signal transfer, enhance cell growth and proliferation, and hence accelerate wound healing. Therefore, water-holding capacity is an important indicator for the biomedical aspect of scaffolds. Figure 6 indicates that the water-holding capacity of the samples grows rapidly with the increase of soak time in the first 120 min, and grows slowly afterwards. After 180 min, the maximum water-holding capacity of G64, G63, G74, G73, G84 and G83 are 265%, 250%, 413%, 385%, 457% and 435%, respectively. This means that the gelatin–GA nanofiber scaffolds have favorable water-holding capacity.

3.7 Moisture retention analysis

Winter finds that wound heals faster with lighter pain and less scars in closed and moist environment than in dry environment [37–38]. Metzger proves that moist dressing has the effect of restraining wound bacteria, promoting cell growth, stimulating blood capillary formation and debridement [39]. The moisture retention in gelatin–GA nanofiber

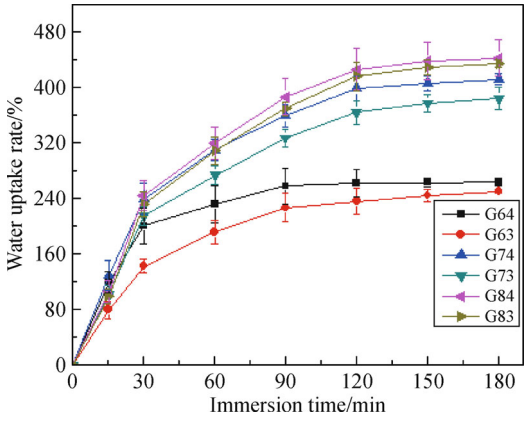

Fig. 6 Water-holding capacity *vs.* soak time curves of gelatin–GA nanofiber scaffolds.

scaffolds can be expressed with water evaporation rate. The higher the evaporation rate the poorer the moisture retention is. Figure 7 reveals that the evaporation rate manifests linear increases in the first 360 min which is rapid dehydration period and the water reduces to more than 82% of its original weight. The main reason is evaporation of free water in opening of gelatin nanofiber scaffolds. The evaporation rate becomes slow after the first 360 min. This is slow dehydration period. The hydrophilic group $-COOH$ and $-NH_2$ in gelatin form hydrogen bond, so molecular chains produce net structures, result in flow resistance and retain water. It also can be seen that the evaporation rate of samples with 1/300 of crosslinking agent (G63, G73 and G83) is higher than that of samples with 1/400 of crosslinking agent (G64, G74 and G84). It means that the higher the GA content the poorer the moisture retention performance. This is because with reaction of GA and gelatin, the hydrophilic groups in large molecules of gelatin are sealed, so the hydrophilic performance of fibrous scaffold weakens.

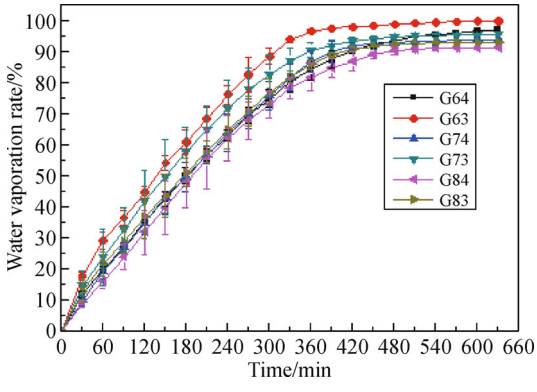

Fig. 7 Water evaporation rate *vs.* time curves of gelatin–GA nanofiber scaffolds.

3.8 Hydrophilic and hydrophobic property analysis

Hydrophilic and hydrophobic property of the scaffold surface has significant influence on adherence, spread and proliferation of cells on the surface [37]. To study the hydrophilic and hydrophobic property, the contact angle of the sample is tested, as is shown in Fig. 8. It can be seen that the contact angles of gelatin–GA nanofiber scaffolds are larger than those of gelatin sample, but all are smaller than 90°. This means that the gelatin–GA nanofiber scaffolds manifest hydrophilic property but their hydrolytic resistance is greatly improved. It also can be seen that contact angles of G63, G73 and G83 are larger than those of G64, G74 and G84. This is because the crosslinking reaction between GA and gelatin greatly reduces the hydrophilic groups in gelatin molecules and enhances the compact degree among molecules, which makes it difficult for water molecules to enter. Therefore, the hydrolytic resistance of the gelatin–GA nanofiber scaffolds is greatly improved compared with that of gelatin one, and this degree of improvement grows with the increase of GA content.

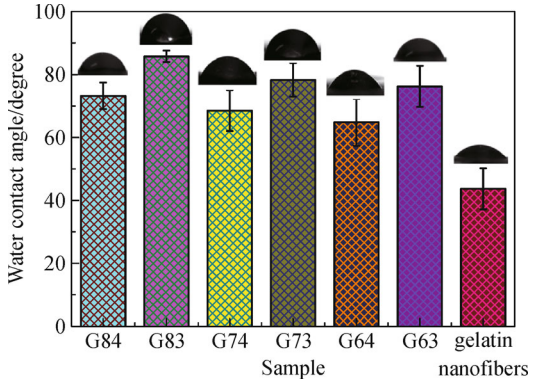

Fig. 8 Contact angles of the gelatin–GA electrospun nanofiber scaffolds.

3.9 Degradation property analysis

Scaffolds for tissue engineering should have certain degradation property to provide enough space for cell growth and tissue formation. There are a number of factors which affect the degradation property such as hydrolysis, dissolution, degeneration and enzymatic catalysis. This research chooses PBS solution which can be used to simulate human body fluid to study the degradation property of the gelatin–GA nanofiber scaffolds. Figure 9 shows that the residual mass of gelatin nanofiber scaffolds at all test time points is obviously smaller than that of the

gelatin–GA ones, which means that the hydrolytic resistance of the latter group is considerably improved. It also can be seen that all the gelatin–GA nanofiber scaffolds have large dissolving-out amount on the first day which is rapid degradation period, and have small dissolving-out amount from the second day to the fifth day which is the slow degradation period. Afterwards, the degradation rate is high. The reason is, in the initial period, gelatin nanofibers are quickly released in the buffer solution. Afterwards, the $-CH=N$ bond generated by crosslinking of GA and gelatin is destroyed. Amino group ($-NH_2$) is regenerated and continuously degrades into the buffer solution but the process considerably decelerates. In the last period, with increased destruction to the crosslinked point, gelatin is dissolved in the buffer solution quickly, so the degradation accelerates. It also reveals that the degradation rate of the gelatin–GA nanofiber scaffolds with 1/300 of GA content (G63, G73 and G83) is lower than that of scaffolds with 1/400 of GA content (G64, G74 and G84), because with more GA the gelatin will have higher crosslinking degree and better hydrolytic resistance.

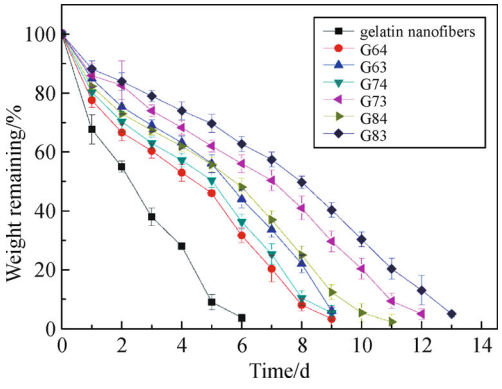

Fig. 9 Degradation curves of the gelatin–GA nanofiber scaffolds.

3.10 Mechanical property analysis

The stress–strain curves of the gelatin–GA nanofiber scaffolds are shown in Fig. 10. The breaking elongation, breaking strength and Young's modulus calculated according to the curve is listed in Table 1. With a low GA content (1/400), the breaking strength and Young's modulus of the gelatin–GA nanofiber scaffolds grows with the increase of gelatin concentration. With a high GA content (1/300), the breaking strength and Young's modulus first grows and then declines with the increase of gelatin concentration. The reason is that the crosslinked gelatin can form a 3D

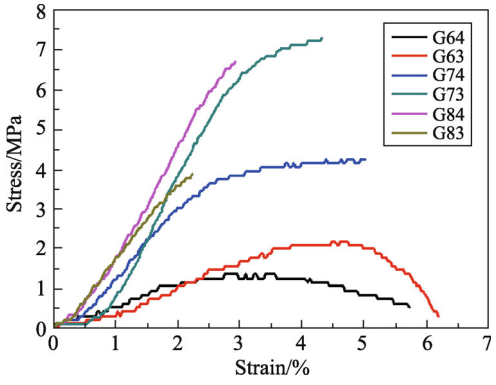

Fig. 10 Stress *vs.* strain curves of the gelatin–GA nanofiber scaffolds.

network structure, and the molecular chain is restrained by crosslinking point and is able to endure large external force. This manifests as higher strength and modulus on a macro level. When the GA content or gelatin solution concentration is low, with the increase of either one, the viscosity of gelatin spinning solution will increase, the density of crosslinked network of molecular chain will increase and the fiber will grow thick (Figs. 2(a)–2(e)). Therefore, both the breaking strength and Young's modulus go up. When the GA content and gelatin concentration is relatively high (such as G83), owing to rapid crosslinking reaction and caking phenomenon, there will be local crosslinking. Meanwhile, because of the high viscosity, the fiber has poor molding (Fig. 2(f)) and hence poor mechanical property of the nanofiber scaffolds. Hence, both the breaking strength and modulus of G83 decrease. It can be seen that, the mechanical property of the gelatin–GA nanofiber scaffolds is adjustable by varying gelatin concentration and crosslinking agent content so as to be better applied for different types of scaffolds for tissue engineering.

3.11 Proliferation and adherence of cells

The activity and proliferation of L929 cells on the sample is shown in Fig. 11. With the extension of culture time, the growth activity of cells on the gelatin–GA nanofiber scaffolds increase to different degrees, manifesting different elevated degrees of light absorbance value tested by the MTT method. At each check time point, the cell proliferation on nanofiber scaffolds is better than that on tissue-culture plates (TCPs), indicating a better proliferation on nanofiber scaffolds. The reason may be that

compared with 2D TCPs, the gelatin–GA nanofiber scaffolds have 3D structure which are similar to that of the natural ECM. The cells can move from the surface to the interior of the scaffolds and hence have more space which is conducive to cell proliferation. In the first five days, there is no evident difference between the states of proliferation on all samples, and on the 7th day the proliferation on G73 and G84 are slightly better than others. It also indicates, with fixed gelatin concentration, when GA content increases from 1/400 to 1/300, there is no obvious change in the cell proliferation on fibrous scaffolds. This means that little change in GA content does not produce evident inhibiting effect on cell activity. The current research is consistent with the reported that a large amount of GA is released from the material when its content is 2.5%, but only a small amount is released when its content is below 1% [36].

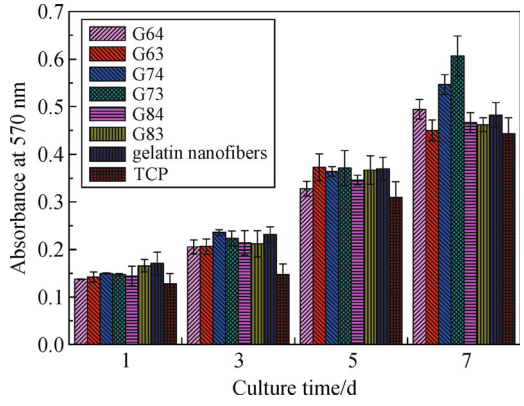

Fig. 11 Proliferation of L929 on TCP and gelatin–GA nanofiber scaffolds after 1, 3, 5 and 7 d.

4 Conclusions

The gelatin–GA nanofiber scaffolds were prepared by adjusting the gelatin concentration and the GA content. The gelatin–GA nanofibers have moderate and uniform crosslinking; the fiber morphology is well retained without adherence, and the porosity is above 80%. The water retention performance, mechanical property, degradation property and thermal resistance of the gelatin–GA nanofibers can be adjusted by varying the gelatin concentration and the GA content. The test results show that G74, G73 and G84, with excellent overall performance such as mechanical property, biocompatibility, hydrolysis resistance, thermal resistance and water retention performance, are expected to be applied in scaffold for tissue engineering, wound repair and drug delivery.

Abbreviations

BR	biological reagent
DMEM	Dulbecco modified Eagle medium
DMSO	dimethyl sulfoxide
DSC	differential scanning calorimetry
ECM	extracellular matrix
FCS	fetal calf serum
FTIR	Fourier transform infrared spectroscopy
GA	glutaraldehyde
HFIP	hexafluoroisopropanol
MTT	3-(4,5-dimethyl-2-thiazolyl)-2,5-diphenyl-2-H-tetrazolium bromide
PBS	phosphate buffer saline
PVA	poly(vinyl alcohol)
SEM	scanning electron microscopy
TCP	tissue-culture plate
XRD	X-ray diffraction

Acknowledgements This research was supported by the National Natural Science Foundation of China (Grant Nos. 31470941 and 31271035), the Innovation Fund Designated for Graduate Students of Donghua University (Item No. CUSF-DH-D-2015032), Science and Technology Commission of Shanghai Municipality (15JC1490100, 15441905100), Ph.D. Programs Foundation of Ministry of Education of China (20130075110005) and light of textile project (J201404), Technology Bureau of Jiaxing City (MTC2012-006, 2011A Y1026), Science and Technology Agency of Zhejiang Province (2012R10012-09, 2010R50012-19). The authors would like to extend their sincere appreciation to the Deanship of Scientific Research at King Saud University for its funding of this research through the research group project No. RGP-201.

References

[1] Matthews J A, Wnek G E, Simpson D G, et al. Electrospinning of collagen nanofibers. Biomacromolecules, 2002, 3(2): 232–238

[2] Ma Z, Kotaki M, Inai R, et al. Potential of nanofiber matrix as tissue-engineering scaffolds. Tissue Engineering, 2005, 11(1–2): 101–109

[3] Sisson K, Zhang C, Farach-Carson M C, et al. Fiber diameters control osteoblastic cell migration and differentiation in electrospun gelatin. Journal of Biomedical Materials Research Part A, 2010, 94A(4): 1312–1320

[4] Zhang S, Huang Y, Yang X, et al. Gelatin nanofibrous membrane fabricated by electrospinning of aqueous gelatin solution for guided tissue regeneration. Journal of Biomedical Materials Research Part A, 2009, 90A(3): 671–679

[5] Choi M O, Kim Y J. Fabrication of gelatin/calcium phosphate composite nanofibrous membranes by biomimetic mineralization. International Journal of Biological Macromolecules, 2012, 50(5): 1188–1194

[6] Baiguera S, Del Gaudio C, Lucatelli E, et al. Electrospun gelatin scaffolds incorporating rat decellularized brain extracellular

matrix for neural tissue engineering. Biomaterials, 2014, 35(4): 1205–1214

[7] Dhandayuthapani B, Krishnan U M, Sethuraman S. Fabrication and characterization of chitosan–gelatin blend nanofibers for skin tissue engineering. Journal of Biomedical Materials Research Part B, 2010, 94B(1): 264–272

[8] Meng Z X, Xu X X, Zheng W, et al. Preparation and characterization of electrospun PLGA/gelatin nanofibers as a potential drug delivery system. Colloids and Surfaces B: Biointerfaces, 2011, 84(1): 97–102

[9] Huang C H, Chi C Y, Chen Y S, et al. Evaluation of proanthocyanidin-crosslinked electrospun gelatin nanofibers for drug delivering system. Materials Science and Engineering C, 2012, 32(8): 2476–2483

[10] Chong E J, Phan T T, Lim I J, et al. Evaluation of electrospun PCL/gelatin nanofibrous scaffold for wound healing and layered dermal reconstitution. Acta Biomaterialia, 2007, 3(3): 321–330

[11] Sisson K, Zhang C, Farach-Carson M C, et al. Evaluation of cross-linking methods for electrospun gelatin on cell growth and viability. Biomacromolecules, 2009, 10(7): 1675–1680

[12] Gomes S R, Rodrigues G, Martins G G, et al. *In vitro* evaluation of crosslinked electrospun fish gelatin scaffolds. Materials Science and Engineering C, 2013, 33(3): 1219–1227

[13] Panzavolta S, Gioffrè M, Focarete M L, et al. Electrospun gelatin nanofibers: optimization of genipin cross-linking to preserve fiber morphology after exposure to water. Acta Biomaterialia, 2011, 7 (4): 1702–1709

[14] Juthamas R, Ratthapol R, Hathairat J, et al. Influences of physical and chemical crosslinking techniques on electrospun type A and B gelatin fiber mats. International Journal of Biological Macromolecules, 2010, 47(4): 431–438

[15] Chen Z, Wang L, Jiang H. The effect of procyanidine crosslinking on the properties of the electrospun gelatin membranes. Biofabrication, 2012, 4(3): 035007

[16] Reddy N, Reddy R, Jiang Q. Crosslinking biopolymers for biomedical applications. Trends in Biotechnology, 2015, 33(6): 362–369

[17] Jalaja K, Kumar P R A, Dey T, et al. Modified dextran cross-linked electrospun gelatin nanofibres for biomedical applications. Carbohydrate Polymers, 2014, 114: 467–475

[18] Jalaja K, James N R. Electrospun gelatin nanofibers: a facile cross-linking approach using oxidized sucrose. International Journal of Biological Macromolecules, 2015, 73: 270–278

[19] Tang C, Saquing C D, Harding J R, et al. *In situ* cross-linking of electrospun poly(vinyl alcohol) nanofibers. Macromolecules, 2010, 43(2): 630–637

[20] Cao M, Chen Z, Tu K, et al. Studies on one-step electrospinning for preparing crosslinked gelatin fibers. Acta Polymerica Sinica, 2009, 9(11): 1157–1161 (in Chinese)

[21] Erencia M, Cano F, Tornero J A, et al. Electrospinning of gelatin fibers using solutions with low acetic acid concentration: Effect of solvent composition on both diameter of electrospun fibers and cytotoxicity. Journal of Applied Polymer Science, 2015, 132(25): 1–11

[22] Zhu X, Cui W, Li X, et al. Electrospun fibrous mats with high porosity as potential scaffolds for skin tissue engineering. Biomacromolecules, 2008, 9(7): 1795–1801

[23] Mei L, Hu D, Ma J, et al. Preparation, characterization and evaluation of chitosan macroporous for potential application in skin tissue engineering. International Journal of Biological Macromolecules, 2012, 51(5): 992–997

[24] Hoque M S, Benjakul S, Prodpran T. Effect of heat treatment of film-forming solution on the properties of film from cuttlefish (*Sepia pharaonis*) skin gelatin. Journal of Food Engineering, 2010, 96(1): 66–73

[25] Chen X, Li W, Shao Z, et al. Separation of alcohol-water mixture by pervaporation through a novel natural polymer blend membrane-chitosan/silk fibroin blend membrane. Journal of Applied Polymer Science, 1999, 73(6): 975–980

[26] Okuyama K. Revisiting the molecular structure of collagen. Connective Tissue Research, 2008, 49(5): 299–310

[27] Chen Z, Wang L, Jiang H. The effect of procyanidine crosslinking on the properties of the electrospun gelatin membranes. Biofabrication, 2012, 4(3): 035007

[28] Amadori S, Torricelli P, Rubini K, et al. Effect of sterilization and crosslinking on gelatin films. Journal of Materials Science: Materials in Medicine, 2015, 26(2): 69–70

[29] Bigi A, Panzavolta S, Rubini K. Relationship between triple-helix content and mechanical properties of gelatin films. Biomaterials, 2004, 25(25): 5675–5680

[30] Ki C S, Baek D H, Gang K D, et al. Characterization of gelatin nanofiber prepared from gelatin–formic acid solution. Polymer, 2005, 46(14): 5094–5102

[31] Song J H, Kim H E, Kim H W. Production of electrospun gelatin nanofiber by water-based co-solvent approach. Journal of Materials Science: Materials in Medicine, 2008, 19(1): 95–102

[32] Ren L, Wang J, Yang F Y, et al. Fabrication of gelatin–siloxane fibrous mats via sol–gel and electrospinning procedure and its application for bone tissue engineering. Materials Science and Engineering C, 2010, 30(3): 437–444

[33] Usha R, Ramasami T. Effect of crosslinking agents (basic chromium sulfate and formaldehyde) on the thermal and thermomechanical stability of rat tail tendon collagen fibre. Thermochimica Acta, 2000, 356(1–2): 59–66

[34] de Carvalho R A, Grosso C R F. Characterization of gelatin based films modified with transglutaminase, glyoxal and formaldehyde.

Food Hydrocolloids, 2004, 18(5): 717–726

[35] Zhang Y Z, Venugopal J, Huang Z M, et al. Crosslinking of the electrospun gelatin nanofibers. Polymer, 2006, 47(8): 2911–2917

[36] Bigi A, Cojazzi G, Panzavolta S, et al. Mechanical and thermal properties of gelatin films at different degrees of glutaraldehyde crosslinking. Biomaterials, 2001, 22(8): 763–768

[37] Winter G D. Some factors affecting skin and wound healing. Journal of Tissue Viability, 2006, 16(2): 20–23

[38] Winter G D, Scales J T. Effect of air drying and dressings on the surface of a wound. Nature, 1963, 197(4862): 91–92

[39] Metzger S. Clinical and financial advantages of moist wound management. Home Healthcare Nurse, 2004, 22(9): 586–590